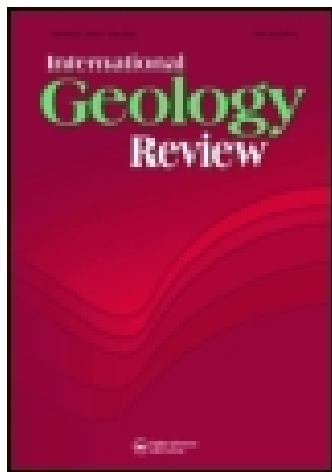


This article was downloaded by: [Selcuk Universitesi]

On: 24 January 2015, At: 21:32

Publisher: Taylor & Francis

Informa Ltd Registered in England and Wales Registered Number: 1072954 Registered office: Mortimer House, 37-41 Mortimer Street, London W1T 3JH, UK



International Geology Review

Publication details, including instructions for authors and subscription information:

<http://www.tandfonline.com/loi/tigr20>

Origin of Triassic granites in central Hunan Province, South China: constraints from zircon U-Pb ages and Hf and O isotopes

Shanling Fu^a, Ruizhong Hu^a, Xianwu Bi^a, Youwei Chen^a, Jiehua Yang^a & Yong Huang^a

^a State Key Laboratory of Ore Deposit Geochemistry, Institute of Geochemistry, Chinese Academy of Sciences, Guiyang 550002, China

Published online: 19 Jan 2015.



CrossMark

[Click for updates](#)

To cite this article: Shanling Fu, Ruizhong Hu, Xianwu Bi, Youwei Chen, Jiehua Yang & Yong Huang (2015): Origin of Triassic granites in central Hunan Province, South China: constraints from zircon U-Pb ages and Hf and O isotopes, International Geology Review, DOI: [10.1080/00206814.2014.996258](https://doi.org/10.1080/00206814.2014.996258)

To link to this article: <http://dx.doi.org/10.1080/00206814.2014.996258>

PLEASE SCROLL DOWN FOR ARTICLE

Taylor & Francis makes every effort to ensure the accuracy of all the information (the "Content") contained in the publications on our platform. However, Taylor & Francis, our agents, and our licensors make no representations or warranties whatsoever as to the accuracy, completeness, or suitability for any purpose of the Content. Any opinions and views expressed in this publication are the opinions and views of the authors, and are not the views of or endorsed by Taylor & Francis. The accuracy of the Content should not be relied upon and should be independently verified with primary sources of information. Taylor and Francis shall not be liable for any losses, actions, claims, proceedings, demands, costs, expenses, damages, and other liabilities whatsoever or howsoever caused arising directly or indirectly in connection with, in relation to or arising out of the use of the Content.

This article may be used for research, teaching, and private study purposes. Any substantial or systematic reproduction, redistribution, reselling, loan, sub-licensing, systematic supply, or distribution in any form to anyone is expressly forbidden. Terms & Conditions of access and use can be found at <http://www.tandfonline.com/page/terms-and-conditions>

Origin of Triassic granites in central Hunan Province, South China: constraints from zircon U–Pb ages and Hf and O isotopes

Shanling Fu, Ruizhong Hu*, Xianwu Bi, Youwei Chen, Jiehua Yang and Yong Huang

State Key Laboratory of Ore Deposit Geochemistry, Institute of Geochemistry, Chinese Academy of Sciences, Guiyang 550002, China

(Received 7 November 2014; accepted 4 December 2014)

Triassic granites crop out extensively in central Hunan Province, South China. Representative granites include the Baimashan, Weishan, and Ziyunshan plutons. Lithologically, these granites mainly comprise biotite monzogranite, two-mica granites, hornblende-biotite granite, hornblende-biotite monzogranite, and garnet-muscovite granite. These granites have *in situ* zircon secondary ion mass spectrum U–Pb ages between 223.2 ± 3.3 and 209.3 ± 4.0 Ma, indicating that they likely formed predominantly in the Late Triassic. These granitic plutons have similar zircon Hf and O isotopic compositions, with $\varepsilon_{\text{Hf}}(t)$ values of -0.8 to -9.0 , two-stage depleted mantle model ages (T_{DM2}) of 1.81–1.31 Ga, and weighted mean of $\delta^{18}\text{O}_{\text{Zrc}}$ values of $8.53 \pm 0.58\%$ to $9.12 \pm 0.28\%$. Combined with U–Pb dating and Hf isotopic data, the elevated and variable $\delta^{18}\text{O}$ and $\varepsilon_{\text{Hf}}(t)$ values of the individual granites indicate that these Triassic granites were likely produced by partial melting of upper Paleoproterozoic to lower Mesoproterozoic metasedimentary rocks and are S-type granites. The variable proportions of inherited zircons in certain samples with U–Pb ages of 627–992 Ma indicate the involvement of lower–middle Neoproterozoic crustal materials during magma crystallization through wall-rock contamination, which resulted in the wide range of isotopic compositions. Underplating of mantle-derived magma may have provided the thermal energy for partial melting of the upper Paleoproterozoic and lower Mesoproterozoic basements, thereby generating these late Triassic granites. The lack of positive $\varepsilon_{\text{Hf}}(t)$ values and high $\delta^{18}\text{O}_{\text{Zrc}}$ values indicate that the contribution of mantle-derived magmas to these granites may be insignificant.

Keywords: Triassic granites; zircon; Hf–O isotopes; magma source; South China

1. Introduction

Extensive Mesozoic magmatism in South China produced one of the largest magmatic provinces in the world (e.g. Zhou and Li 2000; Li and Li 2007). The magmatic activities were mainly concentrated during the Indosinian and Yanshanian; the latter can be further subdivided into early Yanshanian and late Yanshanian (Zhou *et al.* 2006). Associated with considerable granitic intrusions and coeval volcanism, the Yanshanian magmatism has been systematically studied by multidisciplinary approaches and interpreted as an extensional tectonic setting with large-scale mantle–crust interaction in response to the NW-directed subduction of the Pacific Plate (e.g. Faure *et al.* 1996; Lin *et al.* 2000; He *et al.* 2010; He and Xu 2012; Liu *et al.* 2012). In contrast, Indosinian (Triassic) magmatism is not well constrained due to the sporadic distribution and lack of coeval volcanic rocks. Previous studies have suggested that Triassic granites are widespread in South China, especially in Hunan Province, as syn- or late-orogenic products (e.g. Zhou *et al.* 2006; Chen *et al.* 2007a, 2007b; Wang *et al.* 2007b; Zhang *et al.* 2011). However, the timing of the magmatism, lasting from 245 to 200 Ma, is still under debate. Furthermore, the petrogenesis and geodynamic setting of these granitic rocks are also debated, and there are at least three major interpretations: (1) these granites are syn- and post-collisional and are related

to a compressional tectonic regime associated with the collision of the South China block (SCB) and the Indochina block (e.g. Zhou *et al.* 2006; Wang *et al.* 2007b); (2) Li and Li (2007) proposed that a flat-slab subduction orogenic event associated with the paleo-Pacific plate generated these granites; and (3) the Triassic granites were likely formed in an extensional environment related to oblique subduction of the paleo-Pacific plate beneath the SCB (e.g. Wang *et al.* 2005a; Sun *et al.* 2011).

In central Hunan, in the interior of the SCB and far from the continental margins (Figure 1(a)), there are abundant Triassic granites (Figure 1(b)). Although sparse geochronological, geochemical and isotopic data have been preliminarily reported and the petrogenesis of these granites has been discussed (e.g. Ding *et al.* 2006; Wang *et al.* 2007b; Chen *et al.* 2007a, 2007b), the age of these granites, the nature of the source region and the granites' petrogenesis are still controversial. In this work, we combine *in situ* secondary ion mass spectrum (SIMS) zircon U–Pb and O isotopic analyses and LA–MC–ICPMS zircon Lu–Hf isotope analysis on three representative Triassic granites in central Hunan Province in an attempt to better constrain the timing of magmatic activities, the petrogenesis of these granites and the geodynamic setting of Triassic magmatism in South China.

*Corresponding author. Email: huruizhong@vip.gyig.ac.cn

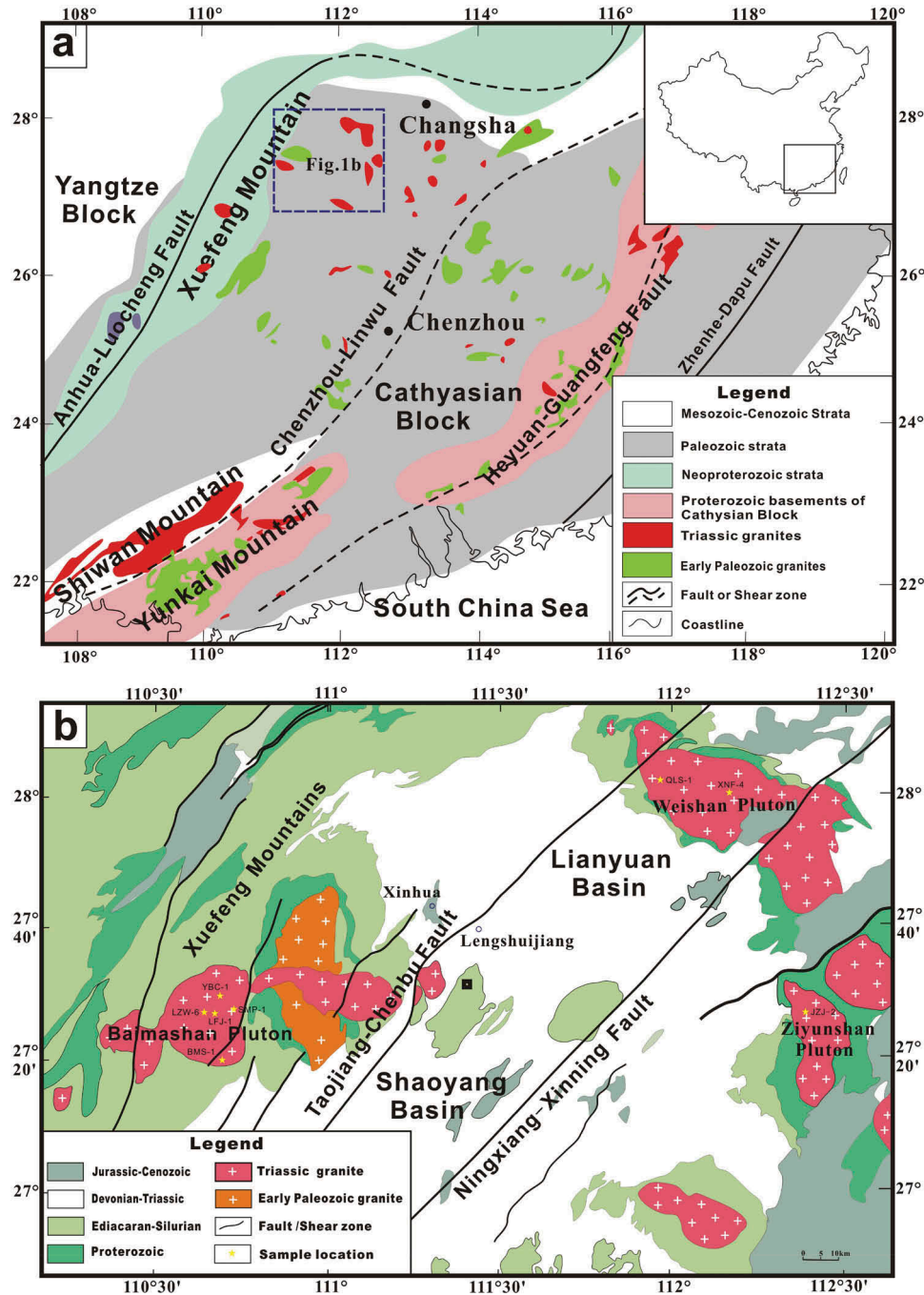


Figure 1. (a) Simplified geological map of the South China Block showing the distribution of Triassic granitic plutons (modified after Wang *et al.* 2007b); (b) geological map showing the Triassic granitic plutons in central Hunan Province (modified after the 1:500,000 geological map of Hunan Province, HNGBMR 1988).

Zircon is a refractory and resistant accessory mineral that preserves a reliable record of oxygen isotopes acquired during magma crystallization (e.g. Valley 2003; Zheng *et al.* 2004, 2007; Valley *et al.* 2005; Kemp *et al.* 2007). Zircon has been shown to be highly retentive of oxygen isotopes (expressed as $\delta^{18}\text{O}$ values) over a wide range of geological conditions (including hydrothermal alteration and magmatic

and granulite-facies metamorphic events) and is suitable for age dating (e.g. Peck *et al.* 2003; Zhao *et al.* 2007; Page *et al.* 2007a, 2007b; Moser *et al.* 2008; Bowman *et al.* 2011). Zircon oxygen isotopes can provide robust constraints on the involvement of magmas from the mantle, upper crust, and lower crust in the generation of granitoids (e.g. Monani and Valley 2001; Valley *et al.* 2005; Kemp *et al.* 2007; Wei

et al. 2008; Wang *et al.* 2013a; Zhao *et al.* 2013a). Zircon Hf isotopes provide another effective approach for constraining the origin of granites due to zircon's high Hf concentrations and resistance to isotopic disturbance (Goodge and Vervoort 2006), and zircon can record isotopic variations during the process of partial melting or fractional crystallization. Therefore, these Hf–O isotopic data, combined with zircon U–Pb dating results, allow us explore the following topics: (1) the precise geochronology of the Triassic granites in South China; (2) the nature of the source of the magmas that generated these granites; and (3) the petrogenesis and geodynamic setting of these Triassic granites.

2. Geological setting

The SCB comprises two distinct tectonic units, the Yangtze block to the northwest and the Cathaysia block to the southeast (Figure 1(a)). The basement of the Yangtze block predominantly consists of Mesoproterozoic to Neoproterozoic metamorphic rocks, including schists, granulites, and amphibolites (Zhou *et al.* 2002; Jiang *et al.* 2009). The basement is overlain by folded Paleozoic and lower Mesozoic shallow-marine strata and Jurassic, Cretaceous, and Cenozoic continental facies strata (Yan *et al.* 2003; Wang *et al.* 2004; Xu *et al.* 2007). In the Cathaysia block, the basement is dominantly 1.9–1.8 Ga sedimentary rocks and Neoproterozoic to lower Paleozoic metamorphic rocks (Yu *et al.* 2005). The Cathaysia block and Yangtze block are generally thought to have collided along the Jiangnan orogen during the late Neoproterozoic (e.g. Wang *et al.* 2007a, 2008a, 2008b; Li *et al.* 2009a; Zhao and Cawood 2012; Yin *et al.* 2013; Zhao and Zhou 2013; Yao *et al.* 2014). Following the Neoproterozoic, the SCB experienced continuous sedimentation for around 400 million years, which was partially controlled by rifting until the Late Ordovician (Wang and Li 2003). Subsequently, the SCB experienced several tectonothermal events in different regions during the early Paleozoic, early Mesozoic, and late Mesozoic (e.g. Ren 1991; Chen 1999; Lin *et al.* 2000; Zhou and Li 2000; Wang *et al.* 2005a; Li and Li 2007; Faure *et al.* 2009; Charvet *et al.* 2010, 2013; Chu and Lin 2014). The early Mesozoic (Triassic) tectonism was the SCB's most important tectonic event and was well developed

throughout the block, generating orogens such as Qinling–Dabie (e.g. Hacker *et al.* 1998; Leech and Webb 2012; references therein) and Songpan–Ganzi (Roger *et al.* 2010; Yan *et al.* 2011). The significant features of this tectonic event were expressed as granitic intrusions, acidic and intermediate volcanism, NE–SW-trending normal and strike-slip faults, over-thrusts, extensional doming, and syn-tectonic terrigenous sedimentation (Chen *et al.* 2014). Triassic granites crop out extensively in central Hunan Province, which is structurally located in the Xuefeng Mountain orogen (Figure 1(b)). These granites intrude the pre-Devonian strata as stocks and batholiths along the margin of the Xiangzhong basin (i.e. Lianyuan basin and Shaoyang basin). In this study, three well-characterized Triassic granitic plutons from central Hunan Province, that is the Baimashan, Weishan, and Ziyunshan plutons (Figure 1(b)), were selected for zircon U–Pb dating and *in situ* Hf–O isotopic analysis. Lithologically, the Baimashan pluton is composed mainly of biotite granodiorites, monzogranites, and two-mica monzogranites; the Weishan pluton is composed of biotite monzogranite and two-mica monzogranite; and the Ziyunshan pluton is composed of hornblende biotite granite and biotite granite (HNGBMR-RGSU 1995a, 1995b; Wang *et al.* 2005b, 2007b). Field investigations have found that these granites exhibit significant zonation: biotite (hornblende) granite – biotite monzogranite – two-mica granites – (tourmaline granite) from margin to core, in which the latter intruded the former. The most common mineral assemblage in these granites is biotite, plagioclase, K-feldspar, quartz with minor amounts of muscovite and hornblende, and accessory minerals such as tourmaline, apatite, zircon, monazite and Fe–Ti oxides. The descriptions of the samples are listed in Table 1.

3. Analytical methods

Eight samples from three granitic plutons were chosen for zircon U–Pb dating and Hf isotopic analyses. The major and trace element analyses (Table 2) show that compositions of the granitic plutons are within the following ranges: SiO₂ = 70.8–73.9 wt.% (one outlier with 64.8 wt.%), K₂O + Na₂O = 7.25–8.62 wt.% and mol (Al₂O₃/(CaO + Na₂O + K₂O)) (A/CNK) = 1.14–1.36

Table 1. Descriptions of representative samples from Triassic granitic plutons in central Hunan Province.

Granitic pluton	Sample no.	Colour	Lithology	Location (GPS)
Baimashan	BMS-01	Grey	Two-mica granite	N27°20'04", E110°42'10"
	LFJ-01	Grey	Tourmaline granite	N27°26'46", E110°40'16"
	LZW-06	Grey	Tourmaline two-mica monzogranite	N27°27'03", E110°39'34"
	SMP-01	Grey	Two-mica monzogranite	N27°27'34", E110°43'40"
	YBC-01	Grey	Two-mica granite	N27°29'36", E110°41'15"
Weishan	QLS-01	Grey	Two-mica granite	N28°01'55", E111°57'48"
	XNF-01	Pink	Two-mica monzogranite	N28°00'13", E112°09'52"
Ziyunshan	JZJ-02	Grey	Biotite granite	N27°26'39", E112°22'49"

Table 2. Major and trace elements of Triassic granitic plutons in central Hunan Province.

Granites	Baimashan pluton					Weishan pluton		Ziyunshan pluton
	BMS-1	LFJ-1	LZW-6	SMP-1	YBC-1	QLS-1	XNF-01	JZJ-02
<i>Major element (%)</i>								
SiO ₂	73.58	64.76	73.55	73.85	73.53	72.44	73.28	70.78
Al ₂ O ₃	13.69	17.41	14.64	14.18	14.02	14.63	14.51	14.72
Fe ₂ O ₃	1.70	2.73	1.19	1.25	1.37	1.56	1.18	2.56
MgO	0.58	0.59	0.34	0.40	0.41	0.42	0.24	0.56
CaO	1.42	1.40	1.30	1.43	1.64	1.65	0.74	2.18
Na ₂ O	3.00	1.59	2.95	2.95	3.13	3.36	3.51	3.25
K ₂ O	3.64	7.02	4.30	4.57	3.87	3.93	4.96	4.38
MnO	0.05	0.06	0.04	0.04	0.04	0.03	0.03	0.04
P ₂ O ₅	0.14	1.06	0.12	0.11	0.10	0.09	0.09	0.09
TiO ₂	0.21	0.15	0.13	0.15	0.16	0.22	0.12	0.31
A/KNC	1.19	1.36	1.23	1.14	1.14	1.14	1.16	1.05
<i>Trace elements (ppm)</i>								
Rb	479	862	456	434	388	239	274	233
Ba	109	255	243	341	233	426	249	384
Th	11.75	13.79	15.72	20.86	20.12	18.53	18.10	23.50
U	8.01	5.65	6.32	7.83	6.02	4.27	6.86	5.78
Ta	4.79	0.70	3.29	2.50	3.11	2.11	2.07	1.82
Nb	16.79	1.50	12.61	12.06	12.50	10.06	11.42	12.47
Ce	34.05	44.40	41.08	62.97	58.84	59.00	53.50	71.80
Sr	32	47	57	68	64	125	67	110
Zr	67	92	85	101	104	130	81	168
Hf	2.28	3.50	2.69	2.98	3.24	3.45	2.41	4.73
Y	14.50	19.37	12.76	14.42	13.98	10.10	16.50	17.80
Yb	1.14	1.49	1.08	1.20	1.21	0.79	1.24	1.52
La	18.54	24.50	23.12	30.04	28.35	31.67	25.40	35.70
Pr	4.06	5.43	4.82	5.94	5.67	5.82	5.63	7.76
Nd	14.12	18.86	16.34	19.88	19.14	18.87	18.90	26.40
Sm	3.24	4.43	3.48	4.01	3.85	3.49	4.55	4.99
Eu	0.28	0.54	0.44	0.52	0.49	0.57	0.38	0.71
Gd	2.34	3.14	2.35	2.56	2.50	2.52	3.57	3.83
Tb	0.52	0.71	0.48	0.52	0.51	0.40	0.62	0.68
Dy	2.75	3.66	2.44	2.65	2.60	1.82	3.01	3.11
Ho	0.53	0.71	0.48	0.53	0.52	0.33	0.54	0.59
Er	1.28	1.74	1.19	1.33	1.32	0.89	1.37	1.78
Tm	0.18	0.25	0.17	0.19	0.19	0.13	0.19	0.25
Lu	0.16	0.20	0.15	0.17	0.17	0.12	0.18	0.24
ΣREE	97.67	129.44	110.39	146.93	139.34	150.39	147.07	179.34

(one outlier with A/CNK = 1.05). These granites fall into the peraluminous field in the mol (Al₂O₃/(Na₂O + K₂O)) (A/NK) versus A/CNK diagram (Figure 2(a)) and alkali feldspar and syenogranite fields in the quartz, alkali feldspar, Plagioclase (QAP) modal diagram for igneous rocks (Figure 2(b)). All samples have low total rare earth element (REE) contents and are enriched in light REEs (Figure 2(c)). In the primitive mantle-normalized trace element diagram (Figure 2(d)), all samples show similar trace element patterns, including enrichment in high field strength elements, such as Rb, Th, U, K, and Pb, and depletion in large ion lithophile elements, such as Nb, Ta, Sr, Ti and Hf.

Zircon grains were separated from the samples via traditional magnetic and heavy-liquid techniques. More than 1000 zircon grains from each sample were recovered,

and representative zircon grains were handpicked under a binocular microscope and mounted in an epoxy resin disc. These zircons were then polished, coated with gold film, and documented with transmitted and reflected light micrographs and cathodoluminescence (CL) images. The CL images were obtained using a LEO1450VP scanning electron microscope at the Institute of Geology and Geophysics, Chinese Academy of Sciences (IGGCAS), Beijing, to characterize the internal texture of the zircons and to select potential target sites for analyses (i.e. *in situ* U–Pb and Hf and O isotope analyses).

Zircon U–Pb isotopic ratios and U, Th and Pb concentrations were determined using a Cameca IMS-1280 SIMS at the IGGCAS. The U–Th–Pb ratios and absolute abundances were determined relative to standard zircon 91500 (Wiedenbeck *et al.* 1995), analyses of which were

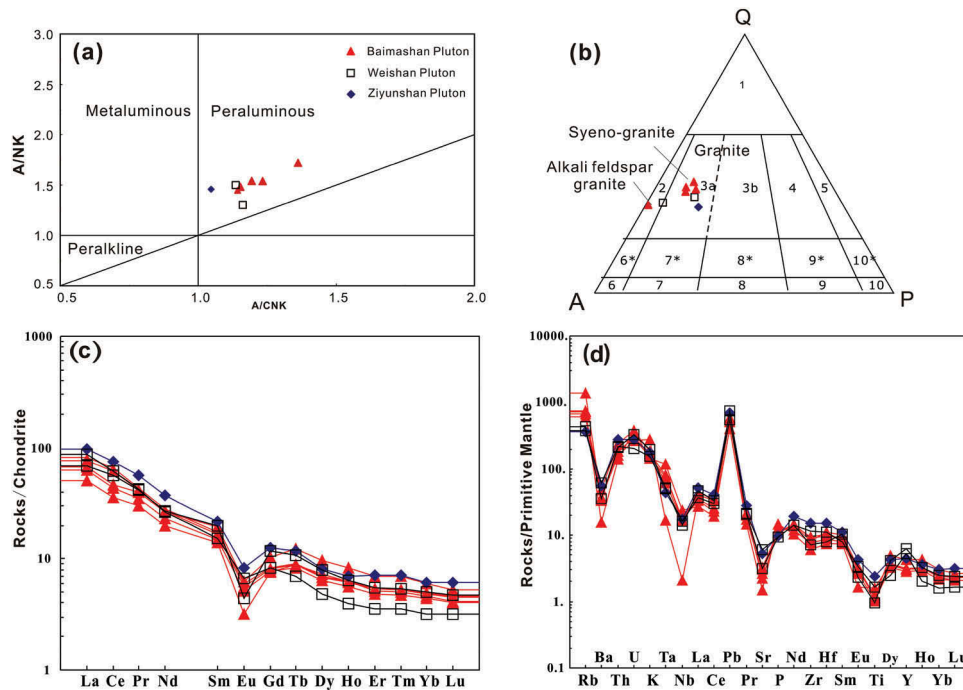


Figure 2. (a) Molar A/NK versus A/CNK diagram; (b) QAP diagram for classification of igneous rocks (based on Streckeisen 1974); (c) chondrite-normalized REE pattern; and (d) primitive mantle-normalized spidergram for Triassic granites in Central Hunan Province. Symbols of diagrams (b), (c) and (d) are the same as diagram (a). The notes of numbers in the diagram (d) refer to Streckeisen (1974).

interspersed with those of unknown grains, using operating and data processing procedures similar to those described in Li *et al.* (2009b). A long-term uncertainty of $\pm 1.5\%$ (1 RSD (relative standard deviation)) in the $^{206}\text{Pb}/^{238}\text{U}$ measurements of the standard zircons was propagated to the unknowns (Li *et al.* 2010), although the measured $^{206}\text{Pb}/^{238}\text{U}$ error in specific sessions was generally approximately $\pm 1\%$ (1 RSD) or less. The measured compositions were corrected for common Pb using non-radiogenic ^{204}Pb . The corrections are sufficiently small as to be insensitive to the choice of common Pb composition, and an average of modern crustal composition (Stacey and Kramers 1975) was used for common Pb based on the assumption that common Pb is largely surface contamination introduced during sample preparation (Chen *et al.* 2014). The uncertainties of individual analyses are reported at the 1-sigma level, and the mean ages of pooled U/Pb (and $^{207}\text{Pb}/^{206}\text{Pb}$) data are reported at the 95% confidence interval. Data reduction was performed using the Isoplot/Ex v.2.49 programs (Ludwig 2001). The SIMS zircon U–Pb isotopic data are presented in Table S1 (see online supplemental material at <http://dx.doi.org/10.1080/00206814.2014.996258>).

The zircon oxygen isotopes were measured using the Cameca IMS-1280 SIMS at the IGGCAS, and the detailed analytical procedures were described in Li *et al.* (2009b). The Cs^+ primary ion beam was accelerated

at 10 kV, with an intensity of approximately 2 nA (Gaussian mode with a primary beam aperture of 200 μm to reduce aberrations) and rastered over a 10 μm area. The spot size was approximately 20 μm in diameter. The normal incidence electron flood gun was used to compensate for sample charging during analysis with a homogeneous electron density over a 30 μm oval area. Negative secondary ions were extracted with a -10 kV potential. The oxygen isotopes were measured using the multi-collection model involving two off-axis Faraday cups. The uncertainties of individual analyses were usually better than ± 0.2 – 0.3% (1RSD). The instrumental mass fractionation factor was corrected using zircon 91500 standards with a $\delta^{18}\text{O}$ value of 9.9‰ (Li *et al.* 2009b). The *in situ* O isotopic data are presented in Table S2 (see online supplemental material at <http://dx.doi.org/10.1080/00206814.2014.996258>).

The *in situ* zircon Hf isotopic analyses were performed on a Neptune multi-collector ICP–MS equipped with a Geolas-193 laser ablation system at the IGGCAS, and the analytical procedures were similar to those described in Wu *et al.* (2006). The Lu–Hf isotopic analyses were obtained largely on the same zircon grains that were previously analysed for O isotopes, with 60 μm diameter ablation pits, an ablation time of 40 s, a repletion rate of 8 Hz, and laser beam energy density of 10 J/cm^2 . During laser ablation analysis, the isobaric interference of ^{176}Lu

on ^{176}Hf is negligible due to extremely low $^{176}\text{Lu}/^{177}\text{Hf}$ ratios in zircon (generally <0.002), whereas the interference of ^{176}Yb on ^{176}Hf is carefully corrected using independent mass bias factors for Hf and Yb. The determined $^{176}\text{Hf}/^{177}\text{Hf}$ value of 0.282303 ± 0.000025 for the zircon standard 91500 is in good agreement with the recorded values (Woodhead *et al.* 2004). The LA-MC-ICPMS zircon Hf isotopic data are presented in Table S3 (see online supplemental material at <http://dx.doi.org/10.1080/00206814.2014.996258>).

4. Results

4.1. SIMS zircon U–Pb ages

4.1.1. Baimashan granitic pluton

Eighteen zircon grains from sample BMS-1 were analysed. Among these, 16 concordant analyses yielded a weighted average $^{206}\text{Pb}/^{238}\text{U}$ age of 214.3 ± 3.4 Ma (95% confidence, mean square weighted deviation (MSWD) = 0.81; Figure 3 (a)), which is considered to be the crystallization age. Two analyses (spots 2 and 7) with U–Pb ages of 680.6 ± 10.0

and 726.6 ± 11.2 Ma were obtained and are interpreted as inherited zircons.

Twenty-two zircon grains from sample LFJ-1 were analysed, and two groups of ages were obtained. The 11 concordant analyses yielded a younger weighted average $^{206}\text{Pb}/^{238}\text{U}$ age of 209.3 ± 4.0 Ma (95% confidence, MSWD = 0.95; Figure 3(b)), which represents the crystallization age. The remaining 11 analyses yielded a broad age range of 882.9–626.8 Ma with an older weighted $^{206}\text{Pb}/^{238}\text{U}$ age of 720 ± 47 Ma (95% confidence, MSWD = 1.12; Figure 3(c)), interpreted as the age of inherited zircons.

Fifteen zircon grains from sample LZW-6 were analysed and yielded a weighted average $^{206}\text{Pb}/^{238}\text{U}$ age of 211.5 ± 4.2 Ma (95% confidence, MSWD = 1.3; Figure 3(d)). We interpreted this age as the crystallization age. This is consistent with the ages of samples BMS-1 and LFJ-1 within uncertainty.

The results of the 19 analysed zircon grains from sample SMP-1 were all concordant and yielded a weighted average $^{206}\text{Pb}/^{238}\text{U}$ age of 215.3 ± 3.1 Ma (95%

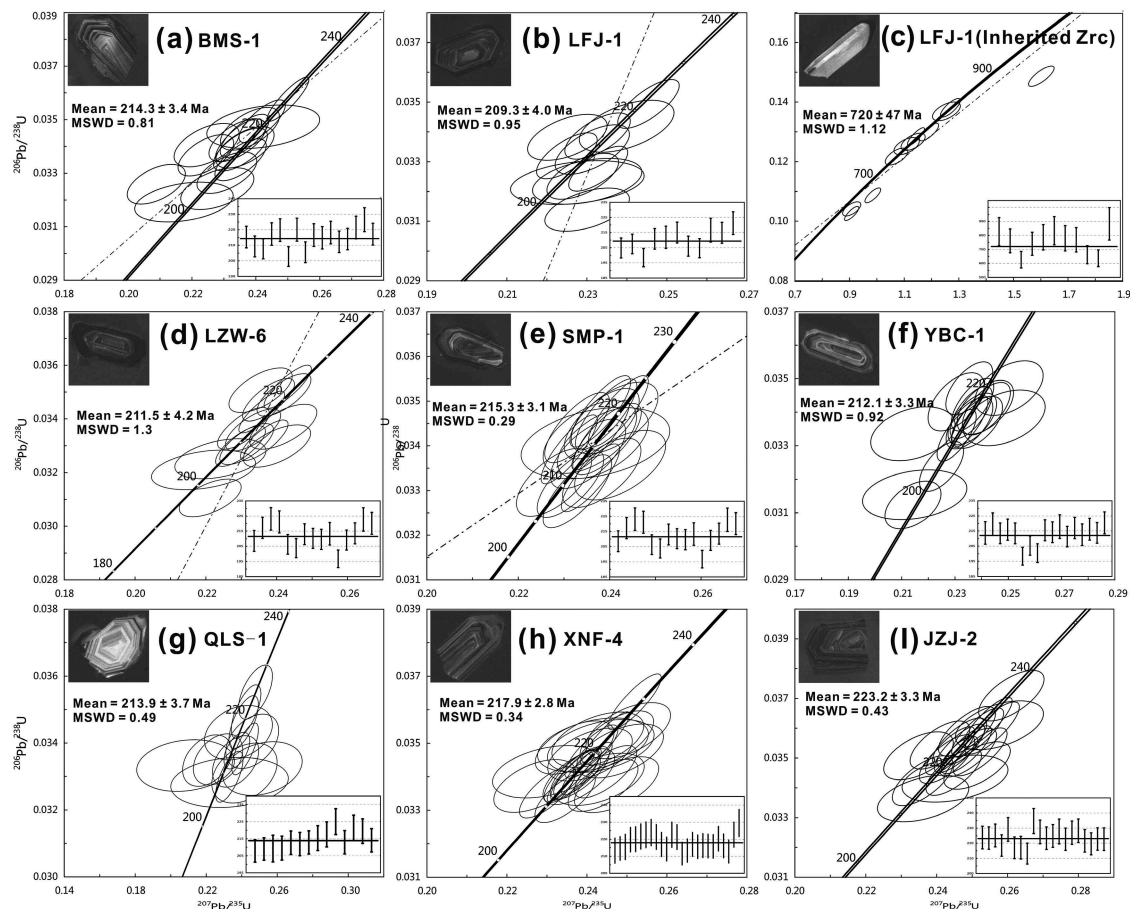


Figure 3. SIMS U–Pb concordant diagram and representative zircon CL images for analysed spots with $^{206}\text{Pb}/^{308}\text{U}$ ages indicated for Triassic granitic plutons in central Hunan Province.

confidence, MSWD = 0.29; Figure 3(e)), which is considered to be the crystallization age.

Seventeen zircon grains from sample YBC-1 were analysed. All the analyses were concordant and yielded a weighted average $^{206}\text{Pb}/^{238}\text{U}$ age of 212.1 ± 3.3 Ma (95% confidence, MSWD = 0.92; Figure 3(f)). This age is interpreted to be the crystallization age and is consistent with those of the above four samples.

4.1.2. Weishan granitic pluton

Seventeen zircon grains from sample QLS-1 were analysed. Among these analyses, 13 analyses were concordant and yielded a weighted average $^{206}\text{Pb}/^{238}\text{U}$ age of 213.9 ± 3.7 Ma (95% confidence, MSWD = 0.49; Figure 3(g)), which is considered to be the crystallization age. This age is consistent with those of the samples collected from the Baimashan granitic pluton. The remaining three analyses (spots 1, 12 and 14) yielded U–Pb ages of 803.2 ± 11.9 , 857.1 ± 12.5 , and 991.7 ± 14.5 Ma, which were interpreted as the ages of inherited zircons.

Twenty-eight zircons from sample XNF-4 were analysed. Twenty-five analyses were concordant, yielding a weighted average $^{206}\text{Pb}/^{238}\text{U}$ age of 217.9 ± 2.8 Ma (95% confidence, MSWD = 0.34; Figure 3(h)). We interpreted this age as the crystallization age, which was slightly older than that of sample QLS-1. Three analyses (spots 2, 10, and 19) yielded U–Pb ages of 826.7 ± 12.2 , 786.8 ± 11.6 , and 850.9 ± 12.4 Ma, respectively, which are considered to be the ages of inherited zircons.

4.1.3. Ziyunshan granitic pluton

Twenty zircons from sample JZJ-2 were analysed. All the analyses were concordant and yielded a weighted average $^{206}\text{Pb}/^{238}\text{U}$ age of 223.2 ± 3.3 Ma (95% confidence, MSWD = 0.43; Figure 3(i)), which is considered to be the crystallization age. This age was slightly older than those of the samples collected from the Baimashan granitic pluton but consistent with that of sample XNF-4 from the Weishan granitic pluton within uncertainty.

4.2. Zircon O isotopes

The zircon grains from the three granites have a narrow range of $\delta^{18}\text{O}_{\text{Zrc}}$ values, with the weighted mean values of single samples varying from $8.53 \pm 0.58\text{‰}$ to $9.12 \pm 0.28\text{‰}$ (Table S2 and Figure 4). Sample JZJ-2 from the Ziyunshan granite has the highest and most uniform $\delta^{18}\text{O}$ values ($9.12 \pm 0.28\text{‰}$), and sample LFJ-1 from the Baimashan granitic pluton has the lowest $\delta^{18}\text{O}$ values ($8.64 \pm 0.53\text{‰}$). Similar oxygen isotopic compositions of the three granites suggest that they may have been derived from a common source. However, the large range of $\delta^{18}\text{O}$

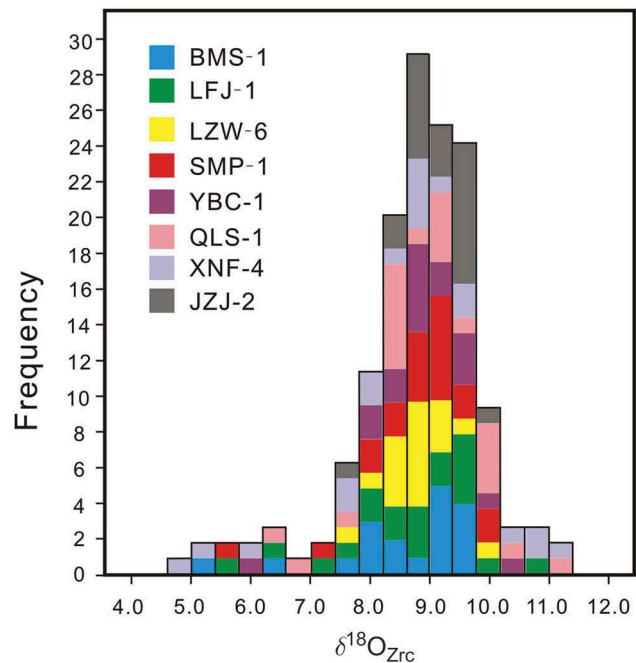


Figure 4. Histogram of $\delta^{18}\text{O}_{\text{Zrc}}$ values for zircons from Triassic granitic plutons in central Hunan Province.

values for single granites indicates a degree of heterogeneity in their source rocks.

4.2.1. Zircons from the Baimashan pluton

The five samples from this pluton have similar oxygen isotopic compositions, with averages of $8.53 \pm 0.58\text{‰}$ (2 SD; $n = 19$) to $8.98 \pm 0.42\text{‰}$ (2 SD; $n = 17$), which are much higher than mantle values. However, there is a wide range of $\delta^{18}\text{O}$ values in individual samples. For example, sample LFJ-1 has a $\delta^{18}\text{O}$ variation of 5.12‰, whereas sample LZW-6 has a relatively small range of 2.32‰. The oxygen isotopic compositions of the Baimashan pluton indicate significant heterogeneity in the source rocks.

4.2.2. Zircons from the Weishan pluton

The two samples from this pluton feature different zircon $\delta^{18}\text{O}$ values. The sample QLS-1 has a broad range of $\delta^{18}\text{O}$ values from 6.21‰ to 11.23‰, with a weighted mean of $8.58 \pm 0.58\text{‰}$ (2 SD; $n = 22$). These data are mainly concentrated in the range of 7.5‰–10‰. The oxygen isotopic values of sample XNF-1 can be divided into two groups: $\delta^{18}\text{O}$ values of 7.56–11.12‰ (weighted mean of $9.35 \pm 0.61\text{‰}$; 2 SD; $n = 16$), which are much higher than mantle values, and $\delta^{18}\text{O}$ values of 4.68‰–5.82‰ (weighted mean of $5.1 \pm 1.4\text{‰}$; 2 SD; $n = 3$), which overlap the mantle $\delta^{18}\text{O}$ values (5.3 ± 0.6 , 2 SD; Valley *et al.* 2005).

4.2.3. Zircons from the Ziyunshan pluton

The oxygen isotopic compositions of zircons in the Ziyunshan granite are higher and more homogenous than the other granites. The $\delta^{18}\text{O}$ values range from 7.49‰ to 9.84‰, with a weighted mean of $9.12 \pm 0.28\%$ (2 SD; $n = 21$).

4.3. Zircon Hf isotopes

The zircon grains from samples BMS-1, LFJ-1, LZW-6, SMP-1 and YBC-1, collected from the Baimashan granitic pluton, have homogeneous Hf isotopic compositions, with $^{176}\text{Hf}/^{177}\text{Hf}$ ratios of 0.282394 to 0.282587, $\varepsilon_{\text{Hf}}(t)$ values of -2.0 to -9.0 and two-stage depleted mantle model ages (T_{DM2}) of 1.38–1.81 Ga. The Ziyunshan pluton (sample JZJ-2) has similar Hf isotopic compositions to the Baimashan pluton, with $^{176}\text{Hf}/^{177}\text{Hf}$ ratios of 0.282533 to 0.282618, $\varepsilon_{\text{Hf}}(t)$ values of -0.8 to -3.8 and T_{DM2} ages of 1.31–1.50 Ga (Table S3 and Figure 5).

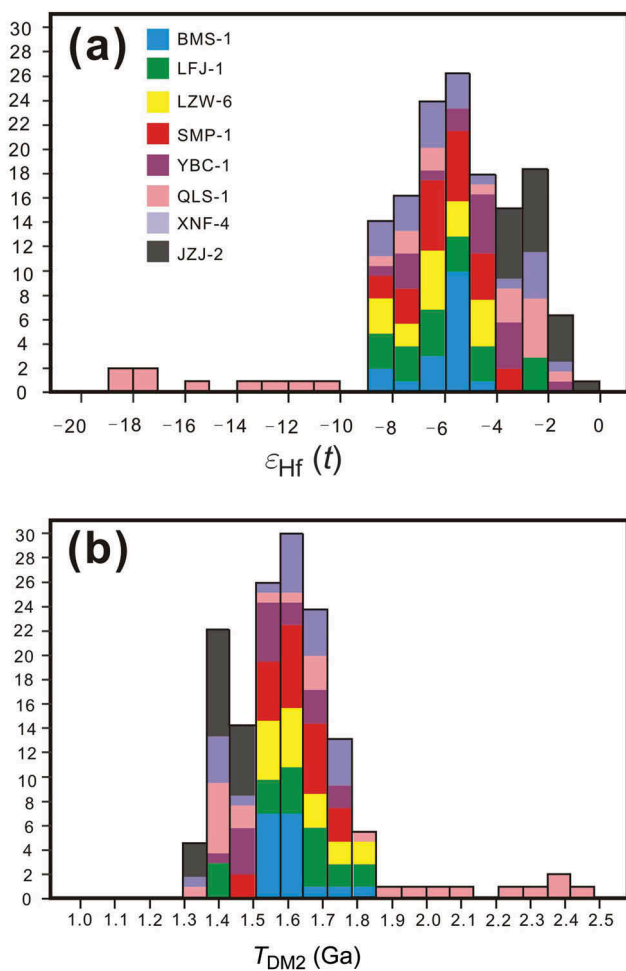


Figure 5. Histograms of $\varepsilon_{\text{Hf}}(t)$ and T_{DM2} values for zircons from Triassic granitic plutons in central Hunan Province.

The zircon grains from sample QLS-1 collected from the Weishan pluton have variable Hf isotopic compositions, with $^{176}\text{Hf}/^{177}\text{Hf}$ ratios of 0.282073–0.282607, $\varepsilon_{\text{Hf}}(t)$ values of -1.4 to -20.3 and T_{DM2} ages of 1.33 Ga–2.51 Ga (Figure 5). However, zircon grains from sample XNF-4 of the Weishan pluton have similar Hf isotopic compositions to the zircon grains from the Baimashan and Ziyunshan granitic plutons, with $^{176}\text{Hf}/^{177}\text{Hf}$ ratios of 0.282409–0.282596, $\varepsilon_{\text{Hf}}(t)$ values of -1.8 to -8.2 and T_{DM2} ages of 1.36–1.76 Ga (Table S3).

5. Discussion

5.1. Geochronology of Triassic granites

Pervious geochronological studies of the Triassic granites in central Hunan Province using K–Ar/Ar–Ar, monazite U–Th–Pb, whole rock Rb–Sr isochrons, and zircon U–Pb methods have produced variable results, with an age range of 267–163 Ma (HNGBMR-RGSU 1995a, 1995b), which is unsuitable for exploring the geochronology of the Triassic granites. In contrast, SHRIMP/LA–ICP–MS zircon U–Pb methods yield a relatively concentrated age range. The data obtained by these methods suggest that the Triassic granites formed in two episodes: 245–228 Ma and 220–206 Ma (e.g. Wang *et al.* 2005b, 2007b; Ding *et al.* 2006; Chen *et al.* 2007a, 2007b). However, our precise SIMS U–Pb dating results do not agree with the previously reported two-episode interpretation. The SIMS zircon U–Pb ages of Triassic granites in central Hunan Province define a cluster of concordant ages with weighted means between 209.3 ± 4.0 and 223.2 ± 3.3 Ma, which are similar to the SIMS U–Pb ages (i.e. 215–225 Ma) of early Mesozoic granites in the Xuefengshan Belt reported by Chu *et al.* (2012b). In addition, the metamorphic rocks of the decollement layer in this region, which were intruded by these granites, yielded monazite U–Pb ages ranging from 226 to 243 Ma (Chu *et al.* 2012a), implying that the formation of these Triassic granites in central Hunan Province occurred after 226 Ma; therefore, older ages may be unreliable. Thus, Triassic granitic magmatism in central Hunan Province likely began since ~ 240 Ma, but the main plutonic phase occurred between 225 and 210 Ma.

5.2. Magma sources: constraints from Hf and O isotopes

Because granites generally inherit geochemical and isotopic characteristics from their sources, the isotope compositions can be used to interpret their likely source reservoir (e.g. Ostendorf *et al.* 2014). The Triassic granites in central Hunan Province are weakly peraluminous granitoids (Table 2; Chen *et al.* 2007a; Wang *et al.* 2007b), which provides a first-order constraint: their sources were likely metasedimentary/metaigneous rocks (e.g. Kalsbeek *et al.*

2001). As stated in Section 1, zircon Hf and O isotopes are very useful in tracing the origins of granites (e.g. Griffin *et al.* 2002; Valley *et al.* 2005; Yang *et al.* 2007; Kemp *et al.* 2007; Bolhar *et al.* 2008). Here, we discuss the constraints provided by Hf and O isotopes on the magma sources of Triassic granites in central Hunan Province.

The oxygen isotopes of igneous zircons that crystallize directly from granitic melts only contain information on the magmatic stage of the granites (e.g. Wang *et al.* 2013a). The oxygen isotope values of mantle-derived zircons, therefore, have a narrow range ($5.3 \pm 0.6\%$, 2σ ; Valley 2003; Valley *et al.* 2005) and are slightly lower than those of mantle-derived magmas (typically $5.7 \pm 0.2\%$; Bindeman 2008). Given that high-temperature closed-system processes in mafic to silicic magmas have little effect on the oxygen isotopic compositions of the resultant rocks, $\delta^{18}\text{O}$ values that extend beyond this range are considered to have been modified by subducted supracrustal materials (e.g. Wan *et al.* 2013). For example, $\delta^{18}\text{O}$ values in zircons greater than approximately 6.3% indicate a $\delta^{18}\text{O}$ -enriched crustal component in the magma from which the zircons crystallized (e.g. Wang *et al.* 2013b), and values above 7.5% are generally attributed to melting or assimilation of supracrustal sources, such as sedimentary rocks (10–30%) or altered volcanic rocks (up to 20%) (Peck *et al.* 2004; Valley *et al.* 2005).

The high weighted mean $\delta^{18}\text{O}$ values of these Triassic granites in central Hunan Province, ranging from $8.53 \pm 0.58\%$ to $9.12 \pm 0.28\%$, allow first-order constraints to be placed on the nature of the granite sources. The oxygen isotope fractionation between zircon and magmas generally increases with the SiO_2 content of the host and is independent of magmatic temperatures (e.g. Valley *et al.* 2003; Zhao and Zheng 2003). Using the linear relationship between $\Delta\delta^{18}\text{O}_{\text{Zrc-WR}}$ and SiO_2 (Lackey *et al.* 2008) of $\Delta\delta^{18}\text{O}_{\text{Zrc-WR}} = -0.0612 * (\text{wt.}\% \text{SiO}_2) + 2.5$, the average $\delta^{18}\text{O}$ values of zircons from granitic plutons in central Hunan Province can be used to estimate the original oxygen isotopic composition of the protolith (Table S2). The protolith appears to be crustal in nature because zircons with $\delta^{18}\text{O}$ values $>6\%$ have not been reported for uncontaminated mantle-derived magmas (e.g. Cavosie *et al.* 2009; Grimes *et al.* 2011; Zhao *et al.* 2013b). Relatively small oxygen isotope fractionations between most minerals and zircons at high temperatures (Valley 2003) require the source rocks to have $\delta^{18}\text{O}$ values higher than the zircons (e.g. Cavosie *et al.* 2011). Sedimentary rocks, such as sandstone, shale, chert, and limestone, as well as metamorphosed equivalents, have high primary $\delta^{18}\text{O}$ values ($>10\%$; Valley *et al.* 2005) and are thus potential sources. In central Hunan Province, the epimetamorphosed Proterozoic basement rocks underlying this region are possible candidates for the high- $\delta^{18}\text{O}$ sources. Magmas with high $\delta^{18}\text{O}$ values may have been produced by the partial melting of these high- $\delta^{18}\text{O}$ rocks, which is also indicated by Hf isotope systematics.

The Hf isotopic compositions of zircon's parental melts are difficult to reset after the Hf isotope system closed and would not be modified by the process of partial melting or fractional crystallization (e.g. Bolhar *et al.* 2008). Therefore, the heterogeneities in the zircon Hf isotope values are consistent with magma sources. As shown in Figure 5, the zircon grains of most samples from the Triassic granites in central Hunan Province feature similar Hf isotopic compositions, that is $\varepsilon_{\text{Hf}}(t)$ values of -0.8 to -9.0 , implying a common parental magma source. Two-stage depleted mantle model ages (T_{DM_2}) of all the analysed zircons range from 1.31 to 1.81 Ga (Figure 5), which are consistent with the dominant crustal ages in this region. In combination with the $\varepsilon_{\text{Hf}}(t)$ values and Hf model ages, a heterogeneous lower crust composed of lower Mesoproterozoic and upper Paleoproterozoic crustal materials is preferred as the potential source of the Triassic granites in central Hunan Province. In addition, the presence of minor inherited zircons with U–Pb ages of 626.8 ± 9.4 – 991.7 ± 14.5 Ma indicates the involvement of lower–middle Neoproterozoic crustal materials during magma crystallization.

It is noteworthy that the Hf and O isotopic compositions are similar between plutons. However, the zircons within a single pluton, even within a sample, contain a wide range of isotope compositions. For example, zircons from the sample QLS-1 in Weishan pluton show highly variable Hf and O isotopic compositions, with an $\varepsilon_{\text{Hf}}(t)$ range of -1.4 to -20.3 and a $\delta^{18}\text{O}$ range of 6.21 – 11.23% (Figures 4 and 5(c)). The wide range of isotopic compositions in a single pluton reflects source heterogeneity or contributions from multiple, isotopically distinct components (e.g. Bolhar *et al.* 2008) and precludes a simple evolution by closed-system fractionation processes. Therefore other mechanisms, such as wall-rock reaction, restite separation, or magma mixing should be considered (e.g. Griffin *et al.* 2002; Yang *et al.* 2007). The lack of positive $\varepsilon_{\text{Hf}}(t)$ values and high $\delta^{18}\text{O}$ values preclude the significant incorporation of mantle-derived magma into the magma chamber from which these Triassic granites were derived. There is no clear correlation between Hf and O isotopes (Figure 6), which also indicates that the magma mixing may be insignificant with regard to the wide range of isotopic compositions. Restite separation is also unlikely to produce these variations because, in principle, the restite (source rock remnants) and the magma would be expected to be similar isotopic compositions (e.g. Griffin *et al.* 2002). Instead, reactions between the magma and its wall-rocks, provided that these are not the source rocks of the magma, could generate the observed isotopic variations during crystallization of the magma (e.g. Griffin *et al.* 2002; Yang *et al.* 2007; Heilimo *et al.* 2013). The samples from the Triassic granites in central Hunan Province contain variable proportions of inherited zircons with Neoproterozoic ages of 627–992 Ma (Table S1), potentially indicating wall-rock contamination. A greater number of inherited zircons are

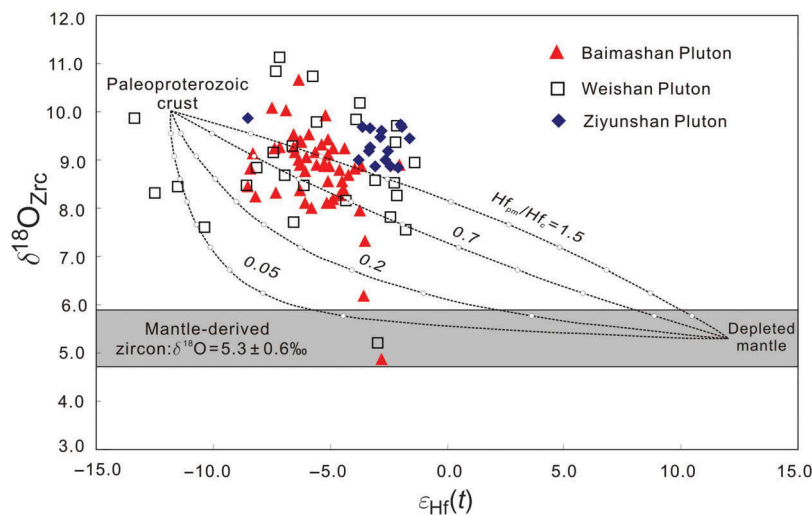


Figure 6. Plots of $\epsilon_{\text{Hf}}(t)$ versus $\delta^{18}\text{O}_{\text{Zrc}}$ data measured on the same zircons in Triassic granitic plutons in central Hunan Province. The dotted lines denote the two-component mixing trends between the mantle and Paleoproterozoic crust-derived magmas. $\text{Hf}_{\text{pm}}/\text{Hf}_{\text{c}}$ is the ratio of Hf concentration in the parental mantle magma (pm) over crustal (c) melt indicated for each curve, and the small open circles on the curves represent 10% mixing increments by assuming that the mantle zircon has $\epsilon_{\text{Hf}} = 12$ and $\delta^{18}\text{O} = 5.3\%$; the Paleoproterozoic crustal zircon has $\epsilon_{\text{Hf}} = -12$ and $\delta^{18}\text{O} = 10\%$.

associated with wider ranges in isotopic compositions (e.g. LFJ-1 and QLS-1; Tables S2 and S3). In contrast, samples with no inherited zircons exhibit a narrow range in isotopic compositions (e.g. JZJ-2 and YBC-1; Tables S2 and S3). The rare zircon grains with low $\delta^{18}\text{O}$ values ($<6.5\%$) were likely produced by the contamination of wall-rocks that may have experienced high-temperature alteration before being incorporated into the magma. Thus, wall-rock contamination may be the dominant mechanism for the wide isotopic ranges.

In summary, the Triassic granites in central Hunan Province have similar zircon Hf and O isotope characteristics. The $\epsilon_{\text{Hf}}(t)$ values are concentrated in the range of -0.8 to -9.0 , and the $\delta^{18}\text{O}$ values range from $8.64 \pm 0.53\%$ to $9.26 \pm 0.18\%$. The negative $\epsilon_{\text{Hf}}(t)$ and high $\delta^{18}\text{O}$ values (Figure 6) suggest that the parental magmas were derived from a pre-existing crustal source that separated from a depleted mantle source during the late Paleoproterozoic to early Mesoproterozoic. In spite of a small difference in the TDM_2 ages, therefore the upper Paleoproterozoic to lower Mesoproterozoic basement metasediments appear to be the dominant source of these Triassic granites in central Hunan Province. In addition, minor Neoproterozoic metasediments intruded by these granites with high $\delta^{18}\text{O}$ values may have been involved in the generation of the Triassic granites.

5.3. Petrogenesis and tectonic setting

The petrogenesis of the Triassic granites in the SCB has long been a matter of debate. The granites' high $\delta^{18}\text{O}$ and negative $\epsilon_{\text{Hf}}(t)$ values (Tables 4 and 5), combined with $\text{A/CNK} > 1.1$

and high $\text{K}_2\text{O} + \text{Na}_2\text{O}$ (Table 2), indicate apparent affinities to S-type granites in geochemical compositions. The zircon U–Pb dating shows that these granites formed in the late Triassic (223–210 Ma). Triassic granites in the SCB were thought to be unrelated to intracontinental collision and subduction due to the absence in SCB of Triassic oceanic basin or subduction involving oceanic and continental plates (e.g. Gilder *et al.* 1996; Rowley *et al.* 1997), the sparse distribution of Triassic granites, and the poor development of coeval volcanic rocks (e.g. Wang *et al.* 2005b; Chen *et al.* 2007a). Certain authors inferred that Triassic granites were derived from crustal sources by decompression melting during the late Triassic in response to the thinning of overthickened crust related to the collision of South China and Indochina (e.g. Ding *et al.* 2006; Chen *et al.* 2007a, 2007b). However, this long-distance effect appears unlikely because these granites are far (>500 km) from the Indosinian suture zone (Chu *et al.* 2012b). Li and Li (2007) proposed a flat-slab subduction model to interpret the intraplate magmatism in South China. However, our Hf and O isotopic results imply a single crustal source for these Triassic granites without input of mantle-derived magmas. Thus, it appears that the flat-slab subduction did not reach the asthenosphere beneath central Hunan Province. Wang *et al.* (2002) proposed that crustal thickening induced by early Triassic intracontinental compression led to the genesis of these granites. The samples are commonly plotted within the field of syn-collisional granite in the plots of tectonic discrimination diagram (Figure 7), also indicating that these granites may have formed in the syn-collisional setting. However, Clemens (2003) argued that a normal geothermal gradient and crustal thickening would fail to provide sufficient heat to partially melt the

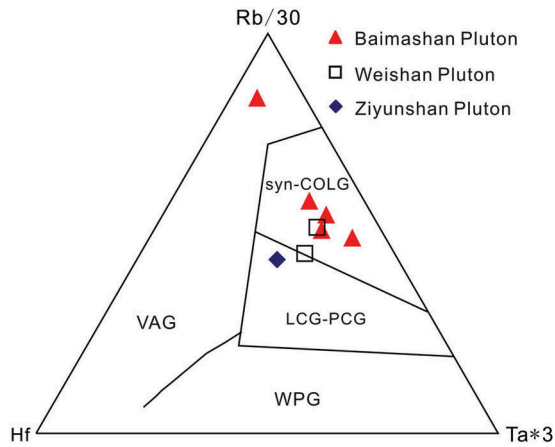


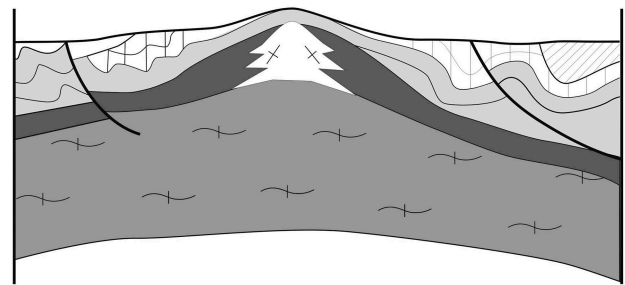
Figure 7. Rb/30 versus Hf versus $3 \times Ta$ diagram of Triassic granitic plutons in central Hunan province (after Pearce *et al.* 1984). Syn-COLG: syn-collisional granites, VAG: volcanic arc granites; WPG: within-plate granites; LCG-PCG: late collisional-post-collisional granites.

crust. It is therefore inferred that underplating of small-scale mantle-derived magmas have heated the Proterozoic meta-sediments and induced the partial melting that led to the genesis of late Triassic granites in central Hunan Province. Evidence for underplating at approximately this time is provided by (1) asthenospheric mantle-derived mafic rocks from Dao County that have been dated to 224–204 Ma (Guo *et al.* 1996, 1997; Dai *et al.* 2008) and the alkaline basalt in Ningyuan County dated to 212–205 Ma (Liu *et al.* 2010) in Hunan Province and (2) a sudden increase in temperature at ca. 225 Ma and subsequent magmatic activity in Hunan Province (Wang *et al.* 2007b). Therefore, a likely scenario of the petrological model can be described as follows (Figure 8): (a) crustal thickening associated with intracontinental orogeny occurred at 243–226 Ma (Chu *et al.* 2012a) and (b) underplating of mantle-derived magma provide thermal energy for partial melting of the thickening crust to generate these late Triassic granites in central Hunan Province. However, the lack of positive $\varepsilon_{Hf}(t)$ values and high $\delta^{18}O$ values (Figure 6) suggested that mantle-derived magma was an insignificant portion of magma source of these granites. This conclusion is also supported by the peraluminous nature and high $K_2O + Na_2O$ content of these granites (Table 2; Wang *et al.* 2007b).

6. Conclusions

- (1) Precise SIMS U–Pb dating results of Triassic granites in central Hunan Province suggest that Triassic granitic magmatism in South China may have begun ca. 240 Ma, but the main plutonic phase occurred between 225 Ma and 210 Ma.

a) Collision and crust thickening at 243–226 Ma



b) Underplating of mantle-derived magma at 225–210 Ma

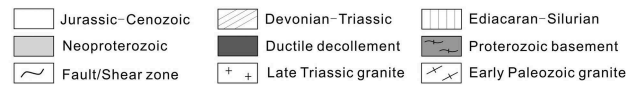
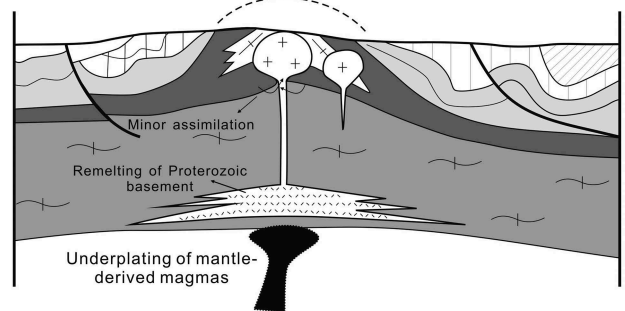


Figure 8. A schematic model for the formation of the late Triassic granitic pluton in central Hunan Province: (a) crustal thickening occurred during 243–226 Ma; (b) underplating of mantle-derived magma heated the thickening crust and induced the partial melting that led to the genesis of these Late Triassic granites in central Hunan Province.

- (2) Zircon grains from Triassic granites in central Hunan Province have similar Hf and O isotopic compositions, with $\varepsilon_{Hf}(t)$ values of -0.8 to -9.0 , T_{DM2} ages of 1.31–1.81 Ga and weighted $\delta^{18}O_{Zrc}$ values of $8.53 \pm 0.58\%$ – $9.12 \pm 0.28\%$. These values indicate that the Triassic granites have similar source rocks and may have been produced by partial melting of upper Paleoproterozoic to lower Mesoproterozoic basement metasediments. Neoproterozoic metasediments may also have been involved through wall-rock contamination, which is supported by inherited zircons and the broad wide ranges in isotopic compositions.
- (3) Underplating of small-scale mantle-derived magmas may have heated the crust and induced the partial melting that led to the genesis of the Late Triassic granites in central Hunan Province. The lack of positive $\varepsilon_{Hf}(t)$ values and high $\delta^{18}O$ values indicate that the contribution of mantle-derived magmas to these granites may be insignificant.

Acknowledgements

We appreciate the assistance of Prof. Xian-hua Li with U–Pb dating and oxygen isotope analysis by Cameca IMS-1280 SIMS and Prof. Fu-yuan Wu with Hf isotope analysis by Neptune multi-collector ICP–MS equipped with a Geolas-193 laser-ablation system. Prof. Mei-Fu Zhou is gratefully acknowledged for his constructive comments on the manuscript.

Funding

This work was financially supported jointly by the National Basic Research Programme of China (973 Programme) [2014CB440906]; Key Project of Natural Science Foundation of China [41230316].

Supplemental data

Supplemental data for this article can be accessed at <http://dx.doi.org/10.1080/00206814.2014.996258>.

References

- Bindeman, I., 2008, Oxygen isotope in mantle and crustal magmas as revealed by single crystal analysis: *Reviews in Mineralogy & Geochemistry*, v. 69, p. 445–478.
- Bolhar, R., Weaver, S.D., Whitehouse, M.J., Woodhead, J.D., and Cole, J.W., 2008, Sources and evolution of arc magmas inferred from coupled O and Hf isotope systematics of plutonic zircons from the Cretaceous Separation Point Suite (New Zealand): *Earth and Planetary Science Letters*, v. 268, p. 312–324.
- Bowman, J.R., Moser, D.E., Valley, J.W., Wooden, J.L., Kita, N. T., and Mazdab, F.K., 2011, Zircon U–Pb isotope, $\delta^{18}\text{O}$ and trace element response to 80 my of high temperature metamorphism in the lower crust: Sluggish diffusion and new records of Archean Craton formation: *American Journal of Society*, v. 311, p. 719–772.
- Cavosie, A.J., Kita, N.T., and Valley, J.W., 2009, Primitive oxygen isotope-ratio recorded in magmatic zircon from the Mid-Atlantic Ridge: *American Mineralogist*, v. 94, p. 926–934.
- Cavosie, A.J., Valley, J.W., Kita, N.T., Spicuzza, K.J., Ushikubo, T., and Wilde, S.A., 2011, The origin of high $\delta^{18}\text{O}$ zircons: Marbles, megacrysts, and metamorphism: *Contributions to Mineralogy and Petrology*, v. 162, p. 961–974.
- Charvet, J., 2013, The Neoproterozoic–Early Paleozoic tectonic evolution of the South China Block: An overview: *Journal of Asian Earth Sciences*, v. 74, p. 198–209.
- Charvet, J., Shu, L.S., Faure, M., Choulet, F., Wang, B., Lu, H.F., and Breton, N.L., 2010, Structural development of the Lower Paleozoic belt of South China: Genesis of an intracontinental orogen: *Journal of Asian Earth Sciences*, v. 39, p. 309–330.
- Chen, A., 1999, Mirror-image thrusting in the South China Orogenic Belt: Tectonic evidence from western Fujian, southeastern China: *Tectonophysics*, v. 305, p. 497–519.
- Chen, W.F., Chen, P.R., Huang, H.Y., Ding, X., and Sun, T., 2007a, Chronological and geochemical studies of granite and enclave in Baimashan pluton, Hunan, South China: *Science in China Series D: Earth Science*, v. 11, p. 1606–1627.
- Chen, W.F., Chen, P.R., Zhou, X.M., Huang, H.Y., Ding, X., and Sun, T., 2007b, Single zircon LA-ICP-MS U–Pb dating of the Guandimiao and Wawutang granitic pluton in Hunan, South China and its petrogenetic significance: *Acta Geologica Sinica*, v. 1, p. 81–89.
- Chen, Z.C., Lin, W., Faure, M., Lepvrier, C., Vuong, N.V., and Tich, V.V., 2014, Geochronology and isotope analysis of the Late Paleozoic to Mesozoic granitoids from northeastern Vietnam and implications for the evolution of the South Chin Block: *Journal of Asian Earth Sciences*, v. 86, p. 131–150.
- Chu, Y., Faure, M., Lin, W., Wang, Q.C., and Ji, W.B., 2012a, Tectonics of the Middle Triassic intracontinental Xuefengshan Belt, South China: New insights from structural and chronological constraints on the basal decollement zone: *International Journal of Earth Science*, v. 101, p. 2125–2150.
- Chu, Y., and Lin, W., 2014, Phanerozoic polyorogenic deformation in southern Jiuling massif, northern South China block: Constraints from structural analysis and geochronology: *Journal of Asian Earth Sciences*, v. 86, p. 117–130.
- Chu, Y., Lin, W., Faure, M., Wang, Q.C., and Ji, W.B., 2012b, Phanerozoic tectonothermal events of the Xuefengshan Belt, central South China: Implications from U–Pb age and Lu–Hf determinations of granites: *Lithos*, v. 150, p. 243–255.
- Clemens, J.D., 2003, S-type granitic magmas–petrogenetic issues, models and evidence: *Earth Science Reviews*, v. 61, p. 1–18.
- Dai, B.Z., Jiang, S.Y., Zhao, K.D., and Liu, D.Y., 2008, Geochronology, geochemistry and Hf–Sr–Nd isotopic compositions of Huziyan mafic xenoliths, southern Hunan Province, South China: Petrogenesis and implications for lower crust evolution: *Lithos*, v. 102, p. 65–87.
- Ding, X., Chen, P.R., Chen, W.F., Huang, H.Y., and Zhou, X.M., 2006, Single zircon LA-ICPMS U–Pb dating of Weishan granite (Hunan, South China) and its petrogenetic significance: *Science in China Series D: Earth Science*, v. 8, p. 816–827.
- Faure, M., Shu, L.S., Wang, B., Charvet, J., Choulet, F., and Monié, P., 2009, Intracontinental subduction: A possible mechanism for the Early Paleozoic Orogen of SE China: *Terra Nova*, v. 21, p. 360–368.
- Faure, M., Sun, T., Shu, L., Monié, P., and Charver, J., 1996, Extensional tectonics within a subduction-type orogen. The case study of the Wugongshan dome (Jiangxi Province, southeastern China): *Tectonophysics*, v. 263, p. 77–106.
- Gilder, S.A., Gill, J., Coe, R.S., Zhao, X.X., Liu, Z.W., Wang, G. X., Yuan, K.R., Liu, W.L., Kuang, G.D., and Wu, H.R., 1996, Isotopic and paleomagnetic constraints on the Mesozoic tectonic evolution of South China: *Journal of Geophysics Research*, v. 107, no. B7, p. 16137–16154.
- Goodge, J.W., and Vervoort, J.D., 2006, Origin of Mesoproterozoic A-type granites in Laurentia: Hf isotope evidence: *Earth and Planetary Science Letters*, v. 243, p. 711–731.
- Griffin, W.L., Wang, X., Jackson, S.E., Pearson, N.J., and O'Reilly, S.Y., 2002, Zircon geochemistry and magma mixing, SE China: In situ analysis of Hf isotopes, Tonglu and Pingtan igneous complexes: *Lithos*, v. 61, p. 237–269.
- Grimes, C.B., Ushikubo, T., John, B.E., and Valley, J.W., 2011, Uniformly mantle-like $\delta^{18}\text{O}$ in zircons from oceanic plagiogranites and gabbros: *Contributions to Mineralogy and Petrology*, v. 161, p. 13–33.
- Guo, F., Fan, W.M., Lin, G., and Lin, Y., 1997, Sm–Nd dating and petrogenesis of Mesozoic gabbro xenolith in Daoxian County, Hunan Province: *Chinese Science Bulletin*, v. 42, p. 1661–1663.
- Guo, F., Wu, Y.L., Fan, W.M., and Lin, G., 1996, A petrological study on the gabbro xenolith in Ningyuan–Daoxian, Hunan: *Geotectonic et Metallogenia*, v. 1, p. 38–45. (in Chinese with English abstract)

- Hacker, B., Ratschbacher, L., Webb, L., Ireland, T., Walker, D., and Dong, S.W., 1998, U–Pb zircon ages constrain the architecture of the ultrahigh-pressure Qinling–Dabie Orogen, China: *Earth and Planetary Science Letters*, v. 161, p. 215–230.
- He, Z.Y., and Xu, X.S., 2012, Petrogenesis of the late Yanshanian mantle-derived intrusions in southeastern China: Response to the geodynamics of paleo-Pacific plate subduction: *Chemical Geology*, v. 328, p. 208–221.
- He, Z.Y., Xu, X.S., and Niu, Y., 2010, Petrogenesis and tectonic significance of a Mesozoic granite-syenite-gabbro association from inland South China: *Lithos*, v. 119, p. 621–641.
- Heilimo, E., Halla, J., Andersen, T., and Huhma, H., 2013, Neoproterozoic crustal recycling and mantle metasomatism: Hf–Nd–Pb–O evidence from sanukitoids of the Fennoscandian shield: *Precambrian Research*, v. 228, p. 250–266.
- HNGBMR (Bureau of Geology and Mineral Resources of Hunan Province), 1988, *Regional Geology of the Hunan Province*: Beijing, Geological Publishing House, p. 286–507. [in Chinese with English summary.]
- HNGBMR-RGSU (Regional Geological Survey Unit, Bureau of Geology and Mineral Resources of Hunan Province), 1995a, Geological maps of granitic pluton in Hunan Province: *Hunan Geology*, v. 8, no. Supp., p. 1–73. (in Chinese)
- HNGBMR-RGSU (Regional Geological Survey Unit, Bureau of Geology and Mineral Resources of Hunan Province), 1995b, Distinguishing of unit-ultraunit of granites in Hunan Province and mineralization: *Hunan Geology*, v. 8, no. Supp., p. 1–84. (in Chinese)
- Jiang, Y.H., Jiang, S.Y., Dai, B.Z., Liao, S.Y., Zhao, K.D., and Ling, H.F., 2009, Middle to late Jurassic felsic and mafic magmatism in southern Hunan province, southeast China: Implications for a continental arc to rifting: *Lithos*, v. 107, p. 185–204.
- Kalsbeek, F., Jepsen, H.F., and Nutman, A.P., 2001, From source migmatites to plutons: Tracking the origin of ca. 435Ma S-type granites in the East Greenland Caledonian Orogen: *Lithos*, v. 57, p. 1–21.
- Kemp, A.I.S., Hawkesworth, C.J., Foster, G.L., Paterson, B.A., Woodhead, J.D., Hergt, J.M., Gray, C.M., and Whitehouse, M.J., 2007, Magmatic and crustal differentiation history of granitic rocks from Hf–O isotopes in zircon: *Science*, v. 315, p. 980–983.
- Lackey, J.S., Valley, J.W., Chen, J.H., and Stockli, D.F., 2008, Dynamic magma systems, crustal recycling, and alteration in the central Sierra Nevada batholith: The oxygen isotope record: *Journal of Petrology*, v. 49, p. 1397–1426.
- Leech, M.L., and Webb, L.E., 2012, Is the HP-UHP Hong'an–Dabie–Sulu orogen a piercing point for offset on the Tan-Lu fault? *Journal of Asian Earth Sciences*, v. 63, p. 112–129.
- Li, Q.L., Li, X.H., Liu, Y., Wu, F.Y., Yang, J.H., and Mitchell, R. H., 2010, Precise U–Pb and Th–Pb age determination of kimberlitic perovskites by secondary ion mass spectrometry: *Chemical Geology*, v. 269, p. 396–405.
- Li, X.H., Li, W.X., Wang, X.C., Li, Q.L., Liu, Y., and Tang, G. Q., 2009a, Role of mantle-derived magma in genesis of early Yanshanian granites in the Nanling Range, South China: In situ zircon Hf–O isotopic constraints: *Science in China Series D: Earth Sciences*, v. 39, p. 872–887.
- Li, X.H., Liu, Y., Li, Q.L., Guo, C.H., and Chamberlain, K.R., 2009b, Precise determination of Phanerozoic zircon Pb/Pb age by multicollector SIMS without external standardization: *Geochemistry, Geophysics, Geosystems*, v. 10, p. Q04010. doi:10.1029/2009GC002400
- Li, Z.X., and Li, X.H., 2007, Formation of the 1300-km-wide intracontinental orogen and postmagmatic province in Mesozoic South China: A flat-slab subduction of model: *Geology*, v. 35, p. 179–182.
- Lin, W., Faure, M., Monié, P., Scharer, U., Zhang, L.S., and Sun, Y., 2000, Tectonics of SE China: New insights from the Lushan massif (Jiangxi Province): *Tectonics*, v. 19, p. 852–871.
- Liu, L., Xu, X.S., and Zou, H.B., 2012, Episodic eruptions of the late Mesozoic volcanic sequences in southeastern Zhejiang, SE, China: Petrogenesis and implications for the geodynamics of paleo-Pacific subduction: *Lithos*, v. 154, p. 166–180.
- Liu, Y., Li, T.D., Xiao, C.H., Geng, S.F., Wang, T., and Chen, B. H., 2010, New chronology of the Ningyuan alkali basalt in southern Hunan, China: Evidence from LA-ICP-MS zircon U–Pb dating: *Geological Bulletin of China*, v. 6, p. 833–841. (in Chinese with English abstract)
- Ludwig, K.R., 2001, *User's manual for Isoplot/Ex (rev. 2.49): A geochronological toolkit for Microsoft Excel*: Berkeley, California, Berkeley Geochronology Center, Special Publication, No. 1a., p. 1–55.
- Monani, S., and Valley, J.W., 2001, Oxygen isotope ratios of zircon: Magma genesis of low $\delta^{18}\text{O}$ granites from the British Tertiary Igneous Province, western Scotland: *Earth and Planetary Science Letters*, v. 184, p. 377–392.
- Moser, D.E., Bowman, J.R., Wooden, J.L., Valley, J.W., Mazdab, F.K., and Kita, N.T., 2008, Creation of a continent recorded in zircon zoning: *Geology*, v. 36, p. 239–242.
- Ostendorf, J., Jung, S., Gerdes, J.B., and Hauff, F., 2014, Syn-orogenic high-temperature crustal melting: Geochronological and Nd–Sr–Pb isotope constraints from basement-derived granites (Central Damara Orogen, Namibia): *Lithos*, v. 192–195, p. 21–38.
- Page, F.Z., Fu, B., Kita, N.T., Fournelle, J., Spicuzza, M.J., Schulze, D.J., Viljoen, F., Basei, M.A.S., and Valley, J.W., 2007a, Zircons from kimberlite: New insights from oxygen isotopes, trace elements, and Ti in zircon thermometry: *Geochimica et Cosmochimica Acta*, v. 71, p. 3887–3903. doi:10.1016/j.gca.2007.04.031
- Page, F.Z., Ushikubo, T., Kita, N.T., Riciputi, L.R., and Valley, J. W., 2007b, High-precision oxygen isotope analysis of picogram samples reveals $2\mu\text{m}$ gradients and slow diffusion in zircon: *American Mineralogist*, v. 92, p. 1772–1775. doi:10.2138/am.2007.2697
- Pearce, J.A., Harris, N.B.W., and Tindle, A.G., 1984, Trace element discrimination diagrams for the tectonic interpretation of granitic rocks: *Journal of Petrology*, v. 25, p. 956–983. doi:10.1093/petrology/25.4.956
- Peck, W.H., Valley, J.W., Corriveau, L., Davidson, A., McLelland, J., and Farber, D., 2004, Constraints on terrane boundaries and origin of 1.18 to 1.13 Ga granitoids of the Southern Grenville Province from oxygen isotope ratios of zircon, *in* Tollo, R.P., McLelland, J., Corriveau, L., and Bartholomew, M.J. eds., *Proterozoic evolution of the Grenville orogen in North America*, Memoir, Volume 197: Boulder, Colorado, Geological Society of America, p. 163–181.
- Peck, W.H., Valley, J.W., and Graham, C.M., 2003, Slow oxygen diffusion rates in igneous zircons from metamorphic rocks: *American Mineralogist*, v. 88, p. 1003–1014.
- Ren, J.S., 1991, On the geotectonics of southern China: *Acta Geologica Sinica*, v. 2, p. 111–136.
- Roger, F., Jolivet, M., and Malavieille, J., 2010, The tectonic evolution of the Songpan–Garze (North Tibet) and adjacent

- areas from Proterozoic to Present: A synthesis: *Journal of Asian Earth Sciences*, v. 39, p. 254–269. doi:10.1016/j.jseas.2010.03.008
- Rowley, D.B., Ziegler, A.M., and Nie, G., 1997, Comment on ‘Mesozoic overthrust tectonics in South China’: *Geology*, v. 17, p. 384–386.
- Stacey, J.S., and Kramers, J.D., 1975, Approximation of terrestrial lead isotope evolution by a two-stage model: *Earth and Planetary Science Letters*, v. 26, p. 207–221. doi:10.1016/0012-821X(75)90088-6
- Streckeisen, A.L., 1974, Classification and nomenclature of plutonic rocks. Recommendations of the IUGS subcommission on the systematics of igneous rocks: *Geologische Rundschau*, v. 63, p. 773–785. doi:10.1007/BF01820841
- Sun, Y., Ma, C.Q., Liu, Y.Y., and She, Z.B., 2011, Geochronological and geochemical constraints on the petrogenesis of late Triassic aluminous A-type granites in southeast China: *Journal of Asian Earth Sciences*, v. 42, p. 1117–1131. doi:10.1016/j.jseas.2011.06.007
- Valley, J.W., 2003, Oxygen isotopes in zircon. *Reviews in Mineralogy and Geochemistry*, v. 53, p. 343–385. doi:10.2113/0530343
- Valley, J.W., Bindeman, I.N., and Peck, W.H., 2003, Empirical calibration of oxygen isotope fractionation in zircon: *Geochimica et Cosmochimica Acta*, v. 67, p. 3257–3266. doi:10.1016/S0016-7037(03)00090-5
- Valley, J.W., Lackey, J.S., Cavosie, A.J., Clechenko, C.C., Spicuzza, M.J., Basei, M.A.S., Bindeman, I.N., Ferreira, V. P., Sial, A.N., King, E.M., Peck, W.H., Sinha, A.K., and Wei, C.S., 2005, 4.4 billion years of crustal maturation: Oxygen isotope ratios of magmatic zircon: *Contributions to Mineralogy and Petrology*, v. 150, p. 561–580. doi:10.1007/s00410-005-0025-8
- Wan, Y.S., Zhang, Y.H., Williams, I.S., Liu, D.Y., Dong, C.Y., Fan, R.L., Shi, Y.R., and Ma, M.Z., 2013, Extreme zircon O isotopic compositions from 3.8 to 2.5Ga magmatic rocks from the Anshan Area, North China Craton: *Chemical Geology*, v. 352, p. 108–124. doi:10.1016/j.chemgeo.2013.06.009
- Wang, J., and Li, Z.X., 2003, History of Neoproterozoic rift basins in South China: Implications for Rodinia break-up: *Precambrian Research*, v. 122, p. 141–158.
- Wang, Q., Li, J.W., Jian, P., Zhao, Z.H., Xiong, X.L., Bao, Z.W., Xu, J.F., Li, C.F., and Ma, J.L., 2005a, Alkaline syenites in eastern Cathaysia (South China): Link to Permian-Triassic transtension: *Earth and Planetary Science Letters*, v. 230, p. 339–354. doi:10.1016/j.epsl.2004.11.023
- Wang, S.J., Li, S.G., and Liu, S.A., 2013a, The origin and evolution of low $\delta^{18}\text{O}$ magma recorded by multi-growth zircons in granite: *Earth and Planetary Science Letters*, v. 373, p. 233–241. doi:10.1016/j.epsl.2013.05.009
- Wang, X.L., Zhao, G.C., Zhou, J.C., Liu, Y.S., and Hu, J., 2008a, Geochronology and Hf isotopes of zircon from volcanic rocks of the Shuangqiaoshan Group, South China: Implications for the Neoproterozoic tectonic evolution of the eastern Jiangnan orogen: *Gondwana Research*, v. 14, p. 355–367. doi:10.1016/j.gr.2008.03.001
- Wang, X.L., Zhou, J.C., Griffin, W.L., Wang, R.C., Qiu, J.S., O’Reilly, S.Y., Xu, X.S., Liu, X.M., and Zhang, G.L., 2007a, Detrital zircon geochronology of Precambrian basement sequences in the Jiangnan orogen: Dating the assembly of the Yangtze and Cathaysia Blocks: *Precambrian Research*, v. 159, p. 117–131. doi:10.1016/j.precambres.2007.06.005
- Wang, X.L., Zhou, J.C., Qiu, J.S., and Gao, J.F., 2004, Geochemistry of the Meso- to Neoproterozoic basic-acid rocks from Hunan Province, South China: Implications for the evolution of the western Jiangnan orogen: *Precambrian Research*, v. 135, p. 79–103. doi:10.1016/j.precambres.2004.07.006
- Wang, X.L., Zhou, J.C., Qiu, J.S., Jiang, S.Y., and Shi, Y.R., 2008b, Geochronology and geochemistry of Neoproterozoic mafic rocks from western Hunan, South China: Implications for petrogenesis and post-orogenic extension: *Geological Magazine*, v. 145, p. 215–233. doi:10.1017/S0016756807004025
- Wang, X.L., Zhou, J.C., Wan, Y.S., Kitajima, K., Wang, D., Bonamici, C., Qiu, J.S., and Sun, T., 2013b, Magmatic evolution and crustal recycling for Neoproterozoic strongly peraluminous granitoids from southern China: Hf and O isotopes in zircon: *Earth and Planetary Science Letters*, v. 366, p. 71–82. doi:10.1016/j.epsl.2013.02.011
- Wang, Y.J., Fan, W.M., Liang, X.Q., Peng, T.P., and Shi, Y.R., 2005b, SHRIMP zircon U-Pb geochronology of Indosinian granites in Hunan Province and its petrogenetic implications: *Chinese Science Bulletin*, v. 13, p. 1395–1403.
- Wang, Y.J., Fan, W.M., Sun, M., Liang, X.Q., Zhang, Y.H., and Peng, T.P., 2007b, Geochronological, geochemical and geothermal constraints on petrogenesis of the Indosinian peraluminous granites in the South China Block: A case study in the Hunan Province: *Lithos*, v. 96, p. 475–502. doi:10.1016/j.lithos.2006.11.010
- Wang, Y.J., Zhang, Y.H., Fan, W.M., Xi, X.W., Guo, F., and Lin, G., 2002, Numerical modeling of the formation of Indosinian peraluminous granitoids in Hunan Province: Basaltic underplating versus tectonic thickening: *Science in China Series D: Earth Sciences*, v. 45, p. 1042–1056. doi:10.1007/BF02911241
- Wei, C.S., Zhao, Z.F., and Spicuzza, M.J., 2008, Zircon oxygen isotopic constraint on the sources of late Mesozoic A-type granites in eastern China: *Chemical Geology*, v. 250, p. 1–15. doi:10.1016/j.chemgeo.2008.01.004
- Wiedenbeck, M., Alle, P., Corfu, F., Griffin, W.L., Meier, M., Oberli, F., Vonquadt, A., Roddick, J.C., and Spiegel, W., 1995, Three natural zircon standards for U-Th-Pb, Lu-Hf, trace element and REE analyses: *Geostandards and Geoanalytical Research*, v. 19, p. 1–23. doi:10.1111/j.1751-908X.1995.tb00147.x
- Woodhead, J., Hergt, J., Shelley, M., Eggins, S., and Kemp, R., 2004, Zircon Hf-isotope analysis with an excimer laser, depth profiling, ablation of complex geometries, and concomitant age estimation: *Chemical Geology*, v. 209, p. 121–135. doi:10.1016/j.chemgeo.2004.04.026
- Wu, F.Y., Yang, Y.H., Xie, L.W., Yang, J.H., and Xu, P., 2006, Hf isotopic compositions of the standard zircons and baddeleyites used in U-Pb geochronology: *Chemical Geology*, v. 234, p. 105–126. doi:10.1016/j.chemgeo.2006.05.003
- Xu, D.R., Gu, X.X., Li, P.C., Chen, G.H., Xia, B., Robert, B., He, Z.L., and Fu, G.G., 2007, Mesoproterozoic-Neoproterozoic transition: Geochemistry, provenance and tectonic setting of clastic sedimentary rocks on the SE margin of the Yangtze Block, South China: *Journal of Asian Earth Sciences*, v. 29, p. 637–650. doi:10.1016/j.jseas.2006.04.006
- Yan, D.P., Zhou, M.F., Li, S.B., and Wei, G.Q., 2011, Structural and geochronological constraints on the Mesozoic-Cenozoic tectonic evolution of the Longmen Shan thrust belt, eastern Tibetan Plateau: *Tectonics*, v. 30, p. TC6005. doi:10.1029/2011TC002867
- Yan, D.P., Zhou, M.F., Song, H.L., Wang, X.W., and Malpas, J., 2003, Origin and tectonic significance of a Mesozoic multi-layer over-thrust system within the Yangtze Block (South

- China): *Tectonophysics*, v. 361, p. 239–254. doi:10.1016/S0040-1951(02)00646-7
- Yang, J.H., Wu, F.Y., Wilde, S.A., Xie, L.W., Yang, Y.H., and Liu, X.M., 2007, Tracing magma mixing in granite genesis: In situ U–Pb dating and Hf-isotope analysis of zircons: *Contributions to Mineralogy and Petrology*, v. 153, p. 177–190. doi:10.1007/s00410-006-0139-7
- Yao, J.L., Shu, L.S., Santosh, M., and Zhao, G.C., 2014, Neoproterozoic arc-related mafic-ultramafic rocks and syn-collision granite from the western segment of the Jiangnan Orogen, South China: Constraints on the Neoproterozoic assembly of the Yangtze and Cathaysia Blocks: *Precambrian Research*, v. 243, p. 39–62. doi:10.1016/j.precamres.2013.12.027
- Yin, C.Q., Lin, S.F., Davis, D.W., Xing, G.F., Davis, W.J., Cheng, G.H., Xiao, W.J., and Li, L.M., 2013, Tectonic evolution of the southeastern margin of the Yangtze Block: Constraints from SHRIMP U–Pb and LA-ICP-MS Hf isotopic studies of zircon from the eastern Jiangnan Orogenic Belt and implications for the tectonic interpretation of South China: *Precambrian Research*, v. 236, p. 145–156. doi:10.1016/j.precamres.2013.07.022
- Yu, J.H., Zhou, X., O'Reilly, Y.S., Zhao, L., Griffin, W.L., Wang, R., Wang, L., and Chen, X., 2005, Formation history and protolith characteristics of granulite facies metamorphic rock in Central Cathaysia deduced from U–Pb and Lu–Hf isotopic studies of single zircon grains: *Chinese Science Bulletin*, v. 50, p. 2080–2089. doi:10.1007/BF03322805
- Zhang, F., Wang, Y., Chen, X., Fan, W., Zhang, Y., Zhang, G., and Zhang, A., 2011, Triassic high-strain shear zones in Hainan Island (South China) and their implications on the amalgamation of the Indochina and South China Blocks: Kinematic and $^{40}\text{Ar}/^{39}\text{Ar}$ geochronological constraints: *Gondwana Research*, v. 19, p. 910–925. doi:10.1016/j.gr.2010.11.002
- Zhao, G.C., and Cawood, P.A., 2012, Precambrian geology of China: *Precambrian Research*, v. 222–223, p. 13–54. doi:10.1016/j.precamres.2012.09.017
- Zhao, J.H., and Zhou, M.F., 2013, Neoproterozoic high-Mg basalts formed by melting of ambient mantle in South China: *Precambrian Research*, v. 233, p. 193–205. doi:10.1016/j.precamres.2013.04.017
- Zhao, J.H., Zhou, M.F., and Zheng, J.P., 2013a, Constraints from zircon U–Pb ages, O and Hf isotopic compositions on the origin of Neoproterozoic peraluminous granitoids from Jiangnan Fold Belt, South China: *Contributions to Mineralogy and Petrology*, v. 166, p. 1505–1519.
- Zhao, K.D., Jiang, S.Y., Chen, W.F., Chen, P.R., and Ling, H.F., 2013b, Zircon U–Pb chronology and elemental and Sr–Nd–Hf isotope geochemistry of two Triassic A-type granites in South China: Implication for petrogenesis and Indosinian transtensional tectonism: *Lithos*, v. 160–161, p. 292–306. doi:10.1016/j.lithos.2012.11.001
- Zhao, Z.F., and Zheng, Y.F., 2003, Calculation of oxygen isotope fractionation in magmatic rocks: *Chemical Geology*, v. 193, p. 59–80. doi:10.1016/S0009-2541(02)00226-7
- Zhao, Z.F., Zheng, Y.F., Wei, C.S., and Wu, Y.B., 2007, Post-collisional granitoids from the Dabie orogen in China: Zircon U–Pb age, element and O isotope evidence for recycling of subducted continental crust: *Lithos*, v. 93, p. 248–272. doi:10.1016/j.lithos.2006.03.067
- Zheng, Y.F., Wu, Y.B., Chen, F.K., Gong, B., Li, L., and Zhao, Z.F., 2004, Zircon U–Pb and oxygen isotope evidence for a large-scale $\delta^{18}\text{O}$ depletion event in igneous rocks during the Neoproterozoic: *Geochimica et Cosmochimica Acta*, v. 68, p. 4145–4165. doi:10.1016/j.gca.2004.01.007
- Zheng, Y.F., Zhang, S.B., Zhao, Z.F., Wu, Y.B., Li, X.H., Li, Z.X., and Wu, F.Y., 2007, Contrasting zircon Hf and O isotopes in the two episodes of Neoproterozoic granitoids in South China: Implications for growth and reworking of continental crust: *Lithos*, v. 96, p. 127–150. doi:10.1016/j.lithos.2006.10.003
- Zhou, M.F., Yan, D.P., Kennedy, A.K., Li, Y.Q., and Ding, J., 2002, SHRIMP U–Pb zircon geochronological and geochemical evidence for Neoproterozoic arc-magmatism along the western margin of the Yangtze Block, South China: *Earth and Planetary Science Letters*, v. 196, p. 51–67. doi:10.1016/S0012-821X(01)00595-7
- Zhou, X.M., and Li, W.X., 2000, Origin of Late Mesozoic igneous rocks in Southeastern China: Implications for lithosphere subduction and underplating of mafic magmas: *Tectonophysics*, v. 326, p. 269–287. doi:10.1016/S0040-1951(00)00120-7
- Zhou, X.M., Sun, T., Shen, W.Z., Shu, L.S., and Niu, Y.L., 2006, Petrogenesis of Mesozoic granitoids and volcanic rocks in South China: A response to tectonic evolution: *Episodes*, v. 9, p. 26–33.